

Buildings as Batteries - Unlocking Grid Flexibility from Smart Management of Domestic Heating

A. S. Hedar*, M. Zatti**, and F. Bovera*

*Politecnico di Milano, Department of Energy, (Italy)

** Laboratorio Energia e Ambiente Piacenza, (Italy)

Abstract—The proposed optimization model offers the possibility to find the optimal dispatch of heating units to satisfy the thermal demand of buildings, while simultaneously providing flexibility services by leveraging on the energy stored within the envelope. This enables the aggregation of buildings to participate in Ancillary Services Market (ASM) as a Demand Response (DR) provider. The resulting day-ahead program ensures that the state-of-charge of the building (i.e., its indoor temperature) is maintained at a level that allows decreasing or increasing the consumption as a response to a power regulation request from the operator, while maintaining acceptable thermal comfort conditions to the users. Preliminary results demonstrate the available flexibility potential from three different building types under diverse weather conditions, with smart management of the consumption trajectory while saving on operational costs.

Index Terms—Demand side management, HVAC system, Building thermal inertia, Operational optimization.

I. NOMENCLATURE

Abbreviations

HVAC	Heating, Ventilation and Air Conditioning
CR	Capacity Retention
HP	Heat Pump
DAM	Day-Ahead Market

Indexes/ Sets

$t \in T$	Set of timesteps in one day of 15 minutes each
$t \in \tau \subseteq T$	Set of timesteps of availability periods, a subset of T
$tt \in T_t^{CR}$	Set of timesteps counting the minimum CR provision time starting time step $t \in \tau$
$g \in G$	Set of all heating units, a superset of fuel consuming and electricity consuming units
$\supseteq G^f \cup G^{el}$	

Variables

$in_{g,t}^{el}$	Input electricity for heating unit $g \in G^{el}$ at time $t \in T$
$in_{g,t}^{fuel}$	Input fuel for heating unit $g \in G^f$ at time $t \in T$
$q_{g,t}^{gen}$	Generated heat from unit $g \in G$ at time $t \in T$
$z_{g,t}^{ON}$	On/off binary variable for heating unit $g \in G$ at time $t \in T$
$z_{g,t}^{SU}$	Start-up flag binary variable for unit $g \in G$ at time $t \in T$
q_t^{build}	Heat input to the building at time $t \in T$
T_t^{in}	Indoor temperature of the building at time $t \in T$
$\theta_t^{dev\pm}$	Deviation from legacy comfort setpoint at time $t \in T$
$e_{g,t,tt}^{upCR}$	Electricity consumed by unit $g \in G^{elcons}$ during an up/dw CR call starting $t \in \tau$ and at timestep $tt \in T_t^{CR}$
$e_{g,t,tt}^{dwCR}$	
$q_{g,t,tt}^{gen,upCR}$	Heat generated from unit $g \in G^{elcons}$ during an up/dw CR call starting $t \in \tau$ and at timestep $tt \in T_t^{CR}$
$q_{g,t,tt}^{gen,dwCR}$	
$q_{t,tt}^{build,upCR}$	Heat input to the building in an up/dw CR call starting $t \in \tau$ and at $tt \in T^{CR}$
$q_{t,tt}^{build,dwCR}$	
$T_{t,tt}^{in,upCR}$	Indoor temperature in an up/dw CR call starting $t \in \tau$ and at $tt \in T^{CR}$
$T_{t,tt}^{in,dwCR}$	

II. INTRODUCTION

The necessary decarbonization process demands the reliance on non-programmable renewable energy sources (NP-RES) in the power system which calls for unprecedented attention to grid flexibility and security. The repercussions of the gas crisis of 2022 urged the start of the REPowerEU Plan [1] which aims to push NP-RES penetration in the EU generation mix and to reduce the reliance on imported fossil fuels. To maintain an acceptable level of system adequacy and security as NP-RES penetration increases, the National Regulatory Authorities (NRAs) and Transmission System Operators (TSOs) are changing the design of electricity market to (i) favor the installation of new generation capacity and (ii) promote the participation to balancing markets also from smaller units. The latter is mainly performed through specific experimental projects with relaxed participatory prescriptions and attractive remuneration schemes, paying for both the availability and the actual provision of power regulation [2], [3].

The electrification of thermal demand has the potential of strongly reducing the primary energy consumption of the building sector, which in Europe accounts for 40% of total consumption [4]. This poses however some challenges on local power networks, introducing the need to implement Demand Response (DR) actions: thus, DR from thermal management of buildings has recently been a topic of great interest. The concept of using the thermal mass of the building as a thermal storage, exploiting electric energy feeding heat pumps (HP), is an alternative solution to battery-based systems, known as “Buildings as Batteries” capability [5].

This concept has been explored in literature considering short-term DR applications such as peak shaving. G. Reynders et al. in [6], [7] model the building thermal inertia on Modelica to investigate the potential to couple a PV system with a heat pump and store the excess production for peak shaving. It was found that the main limitation with six building cases was thermal comfort and building geometry. A similar approach, aimed at filling the mismatch caused by intermittent PV generation, is examined by Marta J.N. et al. [8]. They quantified building thermal inertia by fitting a building model on experimental measurements from three case studies. The models could then be used for DR simulations. D. T. Nguyen [9] investigates an optimization framework for electric vehicles (EV) and buildings considering user comfort

preference. A model-predictive controller that takes into account the thermal dynamic model of the building, the HVAC system, EV charging, and grid connections is assessed on a single building and multiple ones showing promising economic benefits.

B. Favre and B. Peupartier [10] propose a dynamic programming controller for shifting peak loads considering a building dynamic thermal model and variable electricity pricing mechanism. They do a comprehensive analysis of the effects of the thermal capacity and the level of insulation in the building. Similarly, Z. Wei and J. Calautit [11] demonstrated a model predictive controller design using TRYNYSYS that simulates the building at a higher level than MATLAB with a Kalman Filter function that maps the heating demand considering meteorological data and variable energy pricing.

A. Thavlov and H. W. Bindner [12] explore an approach for modeling the thermal dynamic behavior of a building via machine-learning-based parameter estimation. They feed the final model into a virtual power plant operated by an external company to allow smart control of the building by reducing consumption during peak hours, the smart system then decides if it can do the reduction as long as it does not violate any system constraint.

Experimental validation of pre-heating and pre-cooling within a DR scheme was envisioned by Y. Chen et al. [13] considering both a thermal storage tank beside the passive storage in the building focusing on the capacity and duration level that could be provided in various scenarios.

Other optimization approaches such as the MILP one proposed by [14] and the MINLP proposed by [15] include the thermal dynamic behavior and storage effect from both the buildings and the district heating network (DHN) while finding the optimal schedule that minimizes the costs. However, they classify flexibility of the system as an intrinsic ability to shift the loads in off-peak hours and/or operating the units in higher loading and accessing better part-load behavior.

Although mentioned in some of the previously cited works, the focus on the ancillary services market participation from building thermal inertia was not considered inside a MILP model formulation. The aim of this research is to fill this gap and develop a tool that unlocks buildings' flexibility considering the regulatory design characteristics of balancing markets.

III. METHODOLOGY

1. Problem Statement

The objective of this work is to exploit the thermal dynamic behavior of the building to unlock flexibility services provision to the TSO according to the current rules set out in Italian balancing markets [2]. This is achieved using a heat pump which converts electrical to thermal energy that can be stored within the building envelope and utilized when needed. More specifically, the considered energy storage effect is achieved by periods of

over and under-consumption in certain hours of the day, emulating the charging-discharging phases of a battery, where internal building temperature is a proxy of the battery state-of-charge (see Fig. 1). The heat pump can be replaced or assisted by an auxiliary boiler fed with natural gas.

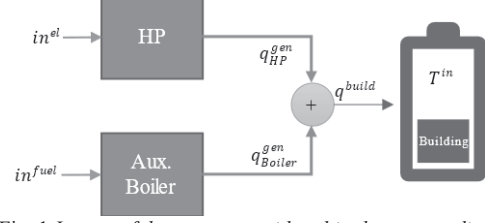


Fig. 1 Layout of the system considered in the case studies.

1. MILP Formulation

The representation of the system has been simplified to include only the heat generation units, the buildings, and a connection to the power and natural gas networks.

1.1. Objective Function

The objective function is to minimize the total daily operational costs (Φ^{fuel} , $\Phi^{electricity}$, $\Phi^{O\&M}$, Φ^{SU}), including the revenues coming from flexibility provision ($CR\ premium$), as well as the penalty assumed for any deviation from the thermal comfort set point ($\theta\ penalty$).

$$\text{minimize } \Phi^{fuel} + \Phi^{electricity} + \Phi^{O\&M} + \Phi^{SU} - CR\ premium + \theta\ penalty$$

$$[\text{€}] \quad \Phi^{fuel} = \sum_T \sum_{G^f} in_{g,t}^{fuel} \cdot c^{fuel} \quad (1)$$

$$[\text{€}] \quad \Phi^{electricity} = \sum_T \sum_{G^{el}} in_{g,t}^{el} \cdot c^{el} \quad (2)$$

$$[\text{€}] \quad \Phi^{O\&M} = \sum_T \sum_G z_{g,t}^{OM} \cdot c_g^{OM} \quad (3)$$

$$[\text{€}] \quad \Phi^{SU} = \sum_T \sum_G z_{g,t}^{SU} \cdot c_g^{SU} \quad (4)$$

$$[\text{€}] \quad CR\ premium = P^{CR} \cdot premium^{CR} \quad (5)$$

$$[\text{€}] \quad \theta\ penalty = \sum_T (\theta_t^{deviation\pm}) \cdot |penalty^\theta| \quad (6)$$

Where Φ^{fuel} , $\Phi^{electricity}$, $\Phi^{O\&M}$, Φ^{SU} are operational costs, $CR\ premium$ is a capacity-based remuneration for the availability to provide flexibility, and the $\theta\ penalty$ is a virtual term to penalize possible thermal discomfort.

1.2. Heating Units

The multi-energy vector model is adapted from [16], [17] and has been simplified to include only the heating vector with two types of units: fuel consuming (G^f), and electricity consuming (G^{el}) units. The heating network is not included, therefore, the output from the two units is fed directly as heat input to the buildings at low temperature without further losses.

1.2.1. Parameters

Each of the generation units is characterized by technical parameters to ensure proper modelling and operation:

- input capacity size ($Size_g$) in $[kW_{input}]$;
- part-load performance coefficients (α_g^{th} , β_g^{th});

- outdoor air temperature effect coefficients for compression-cycle-based units (m_g^{OAT}, q_g^{OAT});
- operational limits (in_g^{min}, in_g^{max}) as percentage of the ($Size_g$);
- limitations on the ramping ($Ramp_g^{lim}$) as percentage of ($Size_g$);
- and allowed number of start-ups (SU_g^{lim}).

1.2.2. Constraints

a) Input Limits

This set of constraints ensures that for each generation unit g during any timestep t , the input is maintained between its minimum and maximum values.

$$[kW] \quad in_{g,t} \geq in_g^{min} \cdot Size_g \cdot z_{g,t}^{ON} \quad \forall G, T \quad (7)$$

$$[kW] \quad in_{g,t} \leq in_g^{max} \cdot Size_g \cdot z_{g,t}^{ON} \quad \forall G, T \quad (8)$$

These constraints also ensure a link between the ON status of the units through the Binary variable ($z_{g,t}^{ON}$).

b) Part-load Performance

The part-load operation of the heating units has been linearized according to the approach explained in [16] for single degree-of-freedom units. The output is a function of the input using two linear coefficients: (α_g^{th}) representing the reference efficiency (or COP in the case of a HP) and (β_g^{th}) capturing the loss term.

$$[kW] \quad q_{g,t}^{gen} = \alpha_g^{th} \cdot in_{g,t}^f + \beta_g^{th} \cdot Size_g \cdot z_{g,t}^{ON} \quad \forall G^f, T \quad (9)$$

In the case of technologies based on compression cycles (e.g., a heat pump), the formula has been corrected to account for the outside air temperature effect by including two extra parameters (m_g^{OAT}) and (q_g^{OAT}).

$$[kW] \quad q_{g,t}^{gen} = \alpha_g^{th} \cdot in_{g,t}^{el} \cdot (m_g^{OAT} \cdot T_t^{out} + q_g^{OAT}) + \beta_g^{th} \cdot Size_g \cdot z_{g,t}^{ON} \quad \forall G^{el}, T \quad (10)$$

c) Ramping and Start-up Limits

First set of constraints ensures that transient operation of unit g at a given timestep t occur within a certain limit for both ramping up (11) and ramping down (12).

$$[kW] \quad in_{g,t} - in_{g,t-1} \leq Ramp_g^{lim} \cdot Size_g \cdot z_{g,t}^{ON} \quad \forall G, T \quad (11)$$

$$[kW] \quad in_{g,t} - in_{g,t+1} \leq Ramp_g^{lim} \cdot Size_g \cdot z_{g,t}^{ON} \quad \forall G, T \quad (12)$$

A binary variable ($z_{g,t}^{SU}$) has been introduced into a logical constraint to flag when the units start up.

$$z_{g,t}^{ON} - z_{g,t-1}^{ON} \leq z_{g,t}^{SU} \quad \forall G, T \quad (13)$$

Once the startup binary flag is defined, we bind the number of start-ups for one day such that for each unit g , at any given timestep t , the sum of startups never exceeds the maximum (SU_g^{lim}).

$$\sum_T z_{g,t}^{SU} \leq SU_g^{lim} \quad \forall G, T \quad (14)$$

1.3. Building Thermal Dynamics

The thermal dynamic model discussed thereafter is based on a linearized single envelope with one indoor temperature in the form of a single-state grey box model adapted from [14] with a simplification to neglect heat

gains and losses except for the overall heat transmission losses to outdoor environment as shown in equation (16). According to [14], a small enough timestep is sufficient to discretize and approximate the physics.

1.3.1. Parameters

The simplified model is characterized by:

- Building heat capacity (C^{th}) in $\left[\frac{kWh}{^\circ C}\right]$;
- Overall thermal loss coefficient (UA) in $\left[\frac{kW}{^\circ C}\right]$.

1.3.2. Constraints

a) Heat balance

The heat balance constraint ensures that at each timestep t , the sum of all the heat contributions from generation units ($q_{g,t}^{gen}$) is equal to the input to the building (q_t^{build}). The heating network is not considered in this work, only the heating units and buildings with no losses.

$$[kW] \quad q_t^{build} = \sum_G q_{g,t}^{gen} \quad \forall T \quad (15)$$

b) Indoor temperature dynamics

From the heat input to the building, the temperature is governed by a simplified model such that at each timestep t , the indoor temperature T_t^{in} changes in the following timestep based on the heat gains and losses and the thermal capacity (C^{th}) of the building.

$$[kW] \quad C^{th} \frac{(T_{t+1}^{in} - T_t^{in})}{\Delta t} = q_t^{building} + UA(T_t^{out} - T_t^{in}) \quad \forall T \quad (16)$$

1.4. Thermal Comfort Management

The thermal comfort strategy for the building is based on fixed indoor temperature setpoint values within the recommended range in the ASHRAE standards [18]. However, for the purpose of unlocking the flexibility within the system, we use the strategy proposed by [14] where a certain flexible band (e.g., $\pm 2^\circ C$) around the setpoint is agreed upon with the user beforehand within a demand-side management scheme.

1.4.1. Parameters

The parameters associated with thermal comfort are:

- Legacy thermal comfort setpoint ($\theta^{in, setpoint}$);
- Min and max bounds to the flexible range ($\theta^{in, flex, min}, \theta^{in, flex, max}$);
- The discomfort ramping/drift limit ($\theta^{in, Ramp, lim}$).

1.4.2. Constraints

a) Indoor temperature limits

To ensure that in each timestep t , the indoor temperature T_t^{in} is never allowed to exceed the flexible range selected, this constraint hard-binds the variable.

$$[^\circ C] \quad \theta^{in, flex, min} \leq T_t^{in} \leq \theta^{in, flex, max} \quad \forall T \quad (17)$$

b) Ramp and drift limits

At any timestep t during the day, the change in temperature is bound to always be lower than drifting or ramping limits to maintain thermal comfort.

$$[^\circ C] \quad T_t^{in} - T_{t-1}^{in} \leq \theta^{in, Ramp, lim} \quad \forall T \quad (18)$$

$$[^\circ C] \quad T_t^{in} - T_{t+1}^{in} \leq \theta^{in, Ramp, lim} \quad \forall T \quad (19)$$

c) Discomfort penalty rule

The allowed temperature range has been expanded to unlock the flexibility within the system. However, in order to minimize the variation in temperature from the legacy comfort condition of fixed temperature, a soft constraint¹ is introduced to penalize any deviation from the selected fixed point either above or below. The deviation variable (slack/surplus) is evaluated at each timestep t as the difference between the indoor temperature and the setpoint temperature.

$$T_t^{in} + \theta_t^{deviation\pm} = \theta^{in,setpoint} \quad \forall T \quad (20)$$

1.5. Capacity Retention Availability

The novelty of this work consists in integrating the demand-side management of the heating demand of the building to the capacity retention market through an electric-driven heat pump. In this chapter, an explanation of the modeling of this interaction is described such that it mirrors what would occur in a real-life situation.

The working principle of the Capacity Retention (CR) market has been adapted from Bovera et al. [19]. A set of constraints is formulated to ensure that the optimal ‘binding’ program takes into account that the system must always be ready to respect any CR call, whether upward or downward, with the requirements that are agreed upon beforehand with the system operator. This means that the model should be able to:

- Correct the unit commitment schedule to maintain a thermal storage level in the building able to provide any possible CR call.
- Ensure that during the real-time rescheduling, all system components will operate within their limits.
- Maintain an acceptable thermal comfort level for the users within the range agreed upon.

1.5.1. Parameters

The capacity retention service is characterized by the set of parameters:

- maximum capacity level that could be requested in a CR call (P^{CR}) in [kW];
- minimum service hold time ($h^{CR,min}$) in [hours];
- start and end hours of the availability periods for the service ($h^{CR,start}, h^{CR,end}$);
- The amount awarded weekly as remuneration of the availability ($premium^{CR}$) in $\left[\frac{\text{€}}{\text{MW-week}}\right]$.

1.5.2. Simulation setup

A new subset τ is defined to include only the timesteps inside the availability periods. It starts at the timestep corresponding to the start hour and ends with the window end.

$$\tau \in [h^{CR,start}, h^{CR,end}] \quad (21)$$

In order to simulate a CR call that starts within a certain timestep ($t \in \tau$) in the availability window and lasts for a duration corresponding to either the minimum service hold time ($\delta^{CR,min}$) or up to the end of the availability window, a new set has been defined to index the CR parameters and variables during the possible calls.

¹ Contrary to the usual (hard) constraints that **must** be satisfied, a soft constraint denotes a **want**, it can be violated but incurs a penalty.

The new set T^{CR} represents the provision time starting right after the activation of the service.

$$T_t^{CR} \in [1, \delta_t^{CR}] \quad (22)$$

The parameter δ_t^{CR} which denotes the duration of a CR call that started at timestep $t \in \tau$ is defined according to a rule that ensures that the duration is always within the availability window as demonstrated mathematically in equation (23), and graphically in Fig. 2.

$$\delta_t^{CR} = \begin{cases} \delta^{CR,min} & , t + \delta^{CR,min} \leq h^{CR,end} \\ h^{CR,end} - t & , t + \delta^{CR,min} > h^{CR,end} \end{cases} \quad (23)$$

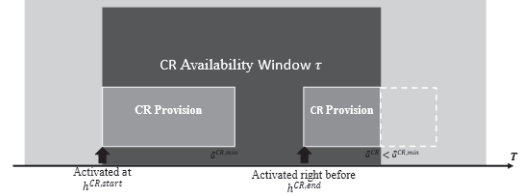


Fig. 2 Visualization of the shrinking simulation time of CR provision at two cases: at the start and near the end of a window.

Each of the simulation variables is then characterized by an index $(t, tt) \in (\tau, T_t^{CR})$ that marks the starting timestep of the call t and the current timestep inside of the simulation tt .

1.5.3. Constraints

All the CR simulation² variables represent possible outcomes, only a simulation of potential calls. They do not represent the actual unit commitment schedule. The simulation variables consider what would occur during a power regulation call starting from the electricity withdrawal by the heat pump $e_{t,tt}^{HP,upCR}, e_{t,tt}^{HP,dwCR}$ for both types of calls up to the indoor temperature $T_{t,tt}^{in,upCR}, T_{t,tt}^{in,dwCR}$ as seen in Fig. 3. This allows a cascaded overview of the system variables, and therefore any operational limits may be enforced during the simulations too. Any violation of the system constraints will result in an infeasibility and consequently modify the real DAM scheduling of the units, thus achieving the required flexibility available as defined.

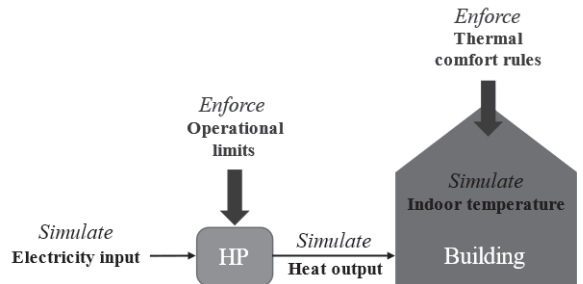


Fig. 3 Graphical representation of the CR simulation and constraints.

a) Electricity input simulation

The goal is to simulate how the electricity input profile would look like during a possible call for CR provision starting from a certain timestep t within the availability time window τ and keeping it running for the minimum service hold duration, corresponding to (T^{CR}) .

² The word “simulation variable” here means they are separate from the real optimal schedule solution; however, they can still affect the solution if any of the constraints is violated.

This is done for each type of CR call: upward corresponding to a reduction in the input and downward with an increase in the input both equal to a capacity level (P^{CR}).

$$[kW] \quad \sum_{G^{el}} e_{g,t,tt}^{upCR} = \left(\sum_{G^{el}} in_{g,t+tt}^{el} \right) - P^{CR} \quad \forall \tau, \forall T^{CR} \quad (24)$$

$$[kW] \quad \sum_{G^{el}} e_{g,t,tt}^{dwCR} = \left(\sum_{G^{el}} in_{g,t+tt}^{el} \right) + P^{CR} \quad \forall \tau, \forall T^{CR} \quad (25)$$

For the sake of simplicity, the equations from now on will be listed only for the upward calls since they are identical for both.

b) Heat balance simulation

This constraint is a computational intermediate step based on the part-load performance maps utilized before in equation (10). To calculate the heat generated during an upward or downward CR call.

$$[kW] \quad q_{g,t,tt}^{gen,upCR} = f(e_{g,t,tt}^{upCR}) \quad \forall G^{el}, \forall \tau, \forall T^{CR} \quad (26)$$

Once the heat output from the HP is calculated, the heat balance is determined taking into account the contribution from the fuel consuming units that are taken directly from the real unaffected schedule.

$$[kW] \quad q_{t,tt}^{build,upCR} = \left(\sum_{G^{el}cons} q_{g,t,tt}^{gen,upCR} \right) + \left(\sum_{G^{T}cons} q_{g,(t+tt-1)}^{generated} \right) \quad \forall \tau, \forall T^{CR} \quad (27)$$

It is important to note that the indexing of any variable of the actual schedule is modified to be concurrent with the simulation as it progresses. The provision of the call is done one timestep after a call has been requested.

c) Thermal dynamics simulation

The last simulation constraint ensures that the temperature profile during the simulation coincides with the variations in the heat provided, which in turn is a result of the CR call being respected. The equations are the same used before for the real schedule in equation (16), concurrent with outdoor temperature.

$$[kW] \quad C^{th} \frac{(T_{t,tt+1}^{in,upCR} - T_{t,tt}^{in,upCR})}{\Delta t} = q_{t,tt}^{building,upCR} + UA \cdot (T_{t+tt}^{outdoor} - T_{t,tt}^{in,upCR}) \quad \forall \tau, \forall T^{CR} \quad (28)$$

d) Heat pump operational limits

Finally, the heat pump is bound to remain within its operational limits during the simulation. The minimum and maximum output are limited in the same way at each simulation timestep (t, tt):

$$[kW] \quad in_{HP}^{min} \cdot Size_{HP} \leq e_{t,tt}^{HP,upCR} \leq in_{HP}^{max} \cdot Size_{HP} \quad \forall \tau, \forall T^{CR} \quad (29)$$

The ramping up and down limits are more particular at the start of the provision and at the end because of how they relate to the real schedule; the general case is the one shown below as the index changes.

$$[kW] \quad e_{t,tt}^{HP,upCR} - e_{t,tt-1}^{HP,upCR} \leq Ramp_{HP}^{lim} \cdot Size_g \quad \forall \tau, \forall T^{CR} \quad (30)$$

$$[kW] \quad e_{t,tt-1}^{HP,upCR} - e_{t,tt}^{HP,upCR} \leq Ramp_{HP}^{lim} \cdot Size_g \quad \forall \tau, \forall T^{CR} \quad (31)$$

e) Building thermal comfort rules

The indoor temperature during the simulation is controlled in the same way as the real schedule and for the sake of simplicity only the upward CR simulation is mentioned in this section.

Minimum and maximum thermal comfort temperatures are always hard constrained in the model even for the simulation values, the constraint is valid for all timesteps.

$$[^\circ C] \quad \theta^{in,flex,min} \leq T_{t,tt}^{in,upCR} \leq \theta^{in,flex,max} \quad \forall \tau, \forall T^{CR} \quad (32)$$

The same goes for the indoor temperature ramping limits constraint.

$$[^\circ C] \quad T_{t,tt}^{in,upCR} - T_{t,tt-1}^{in,upCR} \leq \theta^{in,Ramp,lim} \quad \forall \tau, \forall T^{CR} \quad (33)$$

$$[^\circ C] \quad T_{t,tt}^{in,upCR} - T_{t,tt+1}^{in,upCR} \leq \theta^{in,Ramp,lim} \quad \forall \tau, \forall T^{CR} \quad (34)$$

IV. CASE STUDIES

In this section, the presented model is tested on a single building supplied by heat generation units that are installed directly in the same site assuming the building participates directly to the energy markets. This simplified configuration allows us to better explore and understand the potential of coupling the building storage effect with grid flexibility.

First, two cases are introduced, and the results are discussed in terms of economic and technical performance, with and without flexibility provision. A third case is added for evaluating the effect on flexibility provision of possible building refurbishments.

Some ground assumptions are used for all the cases taken into consideration. A connection to the national electricity and natural gas grid provides the input energy needed to the heat generation units. The units are an electric-driven heat pump and a natural gas auxiliary boiler with their thermal energy output fed directly to the building envelope (see Fig. 1). The injected heat, along with all other gains and losses, affects the indoor temperature gradient and consequently, the thermal comfort of the users within it. To summarize the assumptions:

- The buildings are modelled as one large room with a common indoor temperature and the heat exchange with the outdoor environment is through a singular coefficient.
- The HVAC system is considered as a single unit with the output equal to the sum provided to the building.
- Both Upward CR regulation and Downward CR regulation have the same defined capacity level from each building (e.g., 10 kW)
- There is no limitation on the number of hours with heating allowed to operate during the day.
- The building participates directly in the ancillary services market.

Table I Characterization of the buildings considered in the case studies.

	New Building (B1)	Old Building (B2)	Refurbished (B2R)
Construction year	after 2005	1976-1990	
Building reference picture [18]			
Conditioned floor Area (m^2)	829.4	1088	
Time constant (hour)	37	18	20
Thermal Capacity, C^{th} ($\frac{kWh}{^\circ C}$)	37.32	48.96	48.96
Transmission loss coefficient, UA ($\frac{kW}{^\circ C}$)	1.012	2.676	2.141
Average heating demand (kW_{th})	25.5	66.8	53.41
Available CR power (kW_{el})	D1: 4, D2: 4, D3: 2	D1: 9, D2: 9, D3: 2	D1: 8, D2: 10, D3: 2

1. Building Envelope

Two types of multi-apartment buildings are considered for the case studies. The calculation method and the data elaboration to reach the parameters used are taken from the extensive evaluation done for the TABULA project [20]. The two buildings considered are set in Northern Italy in the Piedmont region: one recently constructed with good insulation, the other is an old building with bad thermal insulation. A third case is added to see the effects of refurbishing the old building with 20% improvement in the insulation as shown in Table I.

2. Heating Units

The units are sized so that either of them is able to supply the end-user with the thermal demand needed (Table I). The demand calculation is based on the simplified RTS approach [21]. The linearized models, operational parameters, and economical parameters are taken from the approach introduced in [17], [22] which are based on data derived from commercially available catalogues for heat pumps and boilers amongst other technologies.

The advantage of the data used is that they are used also for the investment planning problem, hence they can be used for more than one case study depending on the size of the units required to satisfy the building's demand.

3. Flexibility Market Participation

Information about the balancing market and how it works is based on the GAIA model developed in [19] that considers the possible future evolution of the ancillary services market, also based on the Italian pilot project UVAM [2]. It should be noted that the GAIA model considers both the morning peak and afternoon/evening peak time windows, while the pilot projects currently have only the afternoon and evening time divided into two windows. The user participates in a weekly auction awarding the availability (capacity) to provide flexibility in specific time periods. We assume that the auction has already been won and the availability must be respected. Then the aggregator, or balancing service provider (BSP), manages the provision from each building with a certain power level defined beforehand. In our cases, only one building is considered so the optimization defines only one

power level. The Transmission System Operator (TSO) will request an upward call (reduction in energy consumed) or a downward call (increase in energy consumed) which is received 15 minutes ahead and expected to last for a period of up to 2 hours with the periods and remuneration shown in Table II.

Table II CR market conditions considered in the case studies.

	Case study
Availability periods	09:00 – 11:00 16:00 – 20:00
Electricity price	1000 €/MW per week

4. Exogenous Data

In order to run the model, some exogenous data should be included each day, this includes meteorological data and forecasts of the electricity and gas prices.

The temperature profiles are lifted from hourly measurements taken during 2022 in the same geographical location considered, in Northern Italy. In order to have a representation of the winter season, three daily profiles have been selected: an average winter day with moderate temperatures, the coldest day, and a mid-season average day.

Regarding the other exogenous data, the prices for electricity and gas are selected as fixed values for each representative day and taken proportional to the PUN³ in the case of electricity, and average price in the case of natural gas. Both prices are accessed from the website of the operator of the Italian energy markets, GME [23].

Table III Energy prices used in the case studies.

	mild Winter	cold Winter	mid-season
Date	5-Mar	8-Jan	15-Oct
Electricity price	0.40049	0.29185	0.27495
NG price (€/kWh)	0.16681	0.11298	0.10504

V. RESULTS

This chapter presents the results for each building considered with the three representative days from the heating season. The goal is to see the applicability of the proposed Capacity Retention formulation compared with a baseline which doesn't account for energy storage in the building.

³ "Prezzo Unico Nazionale" which is the Italian national price of electrical energy acquired in the energy market managed by GME.

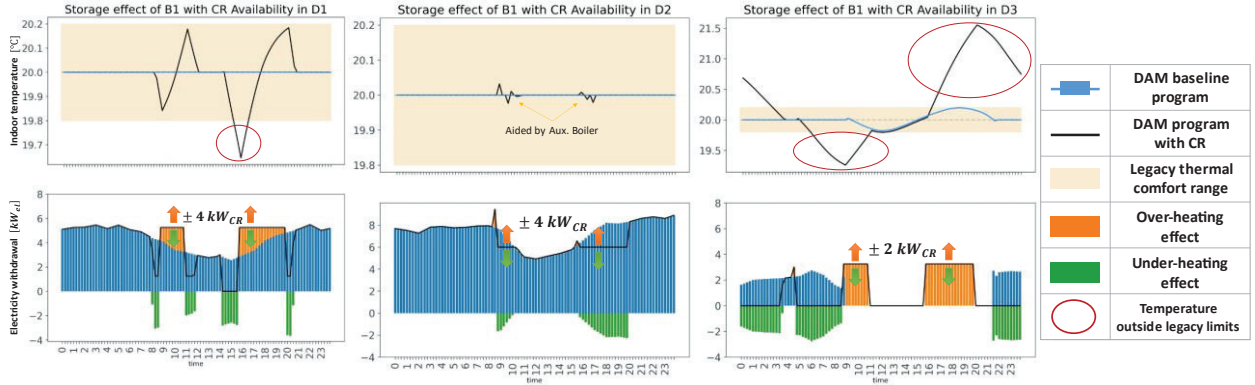


Fig. 4 The over- and under-heating effect in building (B1) from the baseline into the DAM program with CR in three winter days.

1. Case A: New Building

In order to better understand and visualize the effect in the scheduling problem, it is necessary to first define a baseline. For our purpose, the baseline always refers to the optimal schedule without accounting for CR availability compared to the case with CR that could provide any possible future calls. It is important to recall that the consideration of “availability” means that the energy consumption scheduled in the binding day-ahead program is not yet providing any service but is only maintained on stand-by in case of requests.

1.1. Winter Days (D1 and D2)

As shown in Fig. 4, the heat pump program during the availability windows shifts in order to maintain the temperature in an intermediate condition, able to increase or decrease based on the CR calls from the operator. An upward regulation call would be responded to with a modified schedule that reduces the consumption, whereas a Downward regulation call would increase the consumption by storing more heat.

The temperature, if necessary, is allowed to momentarily exceed the thermal comfort range within the flexible band in case of under-heating the building.

The heat pump installed in the building (B1) is able to regulate its electric power consumption for up to $4 kW_{el}$, which if aggregated with other buildings and participating in flexibility provision would generate a negligible amount of money from the availability payment alone, not considering the exchanges of energy following a call.

As expected, the cold winter day (D2) requires more heating energy than the mild winter temperatures. The boiler was deployed at certain timesteps along the day to mitigate the high discomfort levels. It generated $25 kW_{th}$ through the day averaging 5% of the daily thermal demand. The inclusion of the boiler introduced higher costs due to the start-up penalty and more costly energy.

1.2. Mid-season Day (D3)

The mid-season representative day shows a more peculiar behavior compared to cold days since it is usually warm enough not to cause discomfort to the users, hence heating is often turned off. In fact, in 2022 the Italian government restricted that heating would be turned on only after the 15th of October in the cold northern Italian regions in order to reduce natural gas consumption. An important limitation when it comes to the mid-season, is that the

thermal comfort flexible band ($20 \pm 2^\circ\text{C}$) gets violated in the CR simulations considering the same capacity level that was considered in winter and therefore the offered available capacity was reduced. The solutions shown are for a capacity level that is 50% lower.

The case is considered here nonetheless to test a scenario where the energy costs expended are justified in the context of high renewable energy penetration for saving up excess energy during daylight. As we can see in Fig. 4, the heat pump that was turned on during colder periods to maintain acceptable indoor temperatures has been instead shifted to operate in the CR service periods defined.

2. Case B: Old Building

The old building as described in Table I has higher floor area and therefore its thermal capacity is slightly higher, however due to the low insulation levels it has a higher demand and tends to lose heat faster evident in the much lower time constant, compared to the newly constructed building in case B1.

2.1. Winter Days (D1 and D2)

In addition to the obvious difference that the old building with higher thermal demand (2.6 times that of building B1) would be consuming more energy, the intermediate temperature maintained during CR service availability periods caused higher levels of thermal discomfort in the typical winter day (D1) compared with building B1. The alternative would be to deploy the boiler with low output and lower efficiency, causing the daily costs to increase further.

The cold winter day (D2) displayed the same behavior in both buildings, the heat pump is not capable of maintaining acceptable indoor thermal comfort temperature at the same time as it provides capacity availability, therefore the optimal program scheduled the boiler to operate during 4 hours of the day covering between 3 to 30% of the heat demand.

2.1.1. Mid-season Day (D3)

The optimal program for the heating load on a mid-season day with mild temperatures in the case of building B2, is not vastly different from the behavior seen in the new building (B1).

Table IV Key performance indicators of the three building in the mild winter day (D1) compared with their baseline (without CR availability).

	B1 D1		B2 D1		B2R D1	
	binding program	Δ baseline	binding program	Δ baseline	binding program	Δ baseline
Electric consumption ($\frac{kWh}{day}$)	103	-0.36%	273	-0.39%	221	-0.49%
NG consumption ($\frac{kWh}{day}$)	-	-	-	-	-	-
Energy bill costs ($\frac{\epsilon}{day}$)	41	-0.36%	109	-0.39%	88	-0.49%
CR availability ($\frac{\epsilon}{day}$)	0.57	-	1.29	-	1.14	-
Net costs ($\frac{\epsilon}{day}$)	40.76	-1.74%	107.90	-1.56%	87.31	-1.77%
Legacy thermal discomfort duration, peak difference	1.25 (h/day) -0.35 (°C)	-	2.25 (h/day) -0.54 (°C)	-	4.75 (h/day) -0.57 (°C)	-

The main distinction between good and bad insulation is that the loss of heat is faster, and the morning energy expenditure is higher for the old building (see Table IV). The energy scheduled during the capacity retention regulation hours is however maintained at the same level that keeps a temperature that enables power regulation when needed.

2. Case C: Refurbished Building

The main difference is that the building has had an improvement in its insulation of 20% which caused a general reduction in heating demand, and a longer time constant so that heat can be retained for longer periods within the building which allowed higher utilization of the heat pump electricity withdrawal as CR availability compared to before the refurbishment, more specifically, the percentage of offered electric capacity over the heat demand increased from around 13.5% to 15%.

Aside from the energy savings, the behavior differences after the refurbishment are negligible from the point of view of energy storage in the building. The percentage of savings from following the capacity retention availability periods and the revenues from it have a slight improvement from 1.56% to 1.77% reduction.

We believe that the full picture is only accessible following the actual realization of the day which is in the scope of “Rescheduling Optimization.” This allows us to account for the revenues coming from the energy sold or purchased during the power regulation calls in the ASM.

3. Final remarks

The capacity level from each building while satisfying all the requirements from the current projects for including Demand Response into the capacity retention ancillary service ranged between 2 and 10 kW_{el} depending on the day and conditions of the building. In order to get an idea of the scaling this approach would require in order to meet the minimum capacity needed to participate which is for consumption resources 1 MW, we assessed how many buildings it would take for one aggregator to meet the criteria.

Supposing that the aggregator has a range of buildings that is equally distributed (33% each) between the three types and that the winter season is represented only by the mild winter day (D1), it can be estimated that to participate with at least 1 MW_{el} it is required to aggregate a total of 144 buildings. For the cold winter days (D2), only 132 buildings a third from each type is enough to reach

1.01 MW_{el} regulation capacity available. While for the mid-season day (D3), a sum of 501 building stock would be required.

To put this information into perspective, the original study [20] from which the building cases were compiled is based on a building stock sample from one Italian city with a total of 4249 buildings with varying characteristics. This only serves to highlight the potential of the proposed approach if scaled properly.

VI. CONCLUSIONS

The proposed model has demonstrated the capability of thermal energy storage in the building envelope to provide flexibility services to the grid by shifting the consumption, modifying the units program to ensure the availability to regulate the power if needed under the current capacity remuneration schemes from Demand Response.

The MILP model handles the availability by performing a series of simulations of all scenarios in which a capacity regulation call is requested, and by enforcing the system limitations on the scenarios too, the resulting day-ahead program shifts the electrical consumption accordingly. The system limitations include both limitations on the heating units, as well as the indoor temperature thermal comfort rules.

A number of case studies were conducted to evaluate the optimization model and it shows that by allowing a flexible temperature band around the set point, it is possible to meet the criteria to participate in the ancillary services market with the electrification of the thermal units and smart management of their consumption profiles. The modified program had an overall reduction in the daily costs thanks to a small contribution from the availability premium and in some cases a lower electricity consumption at the expense of change in the indoor temperature.

The potential from a single building is promising considering investments in the electrification of the heating infrastructure of buildings. The optimization model sets the stage for integration into bigger frameworks of optimal operation and management of multi-energy systems and energy communities to unlock the potential in our buildings.

For future projects, we think the natural next step could be to either expand the formulation to a district-level with a heating network, or to refine the approach into multi-temporal level with the inclusion of the re-scheduling intra-day optimization problem.

ACKNOWLEDGMENT

Part of the research has received funding from “Ecosystem for Sustainable Transition in Emilia-Romagna,” project funded by European Union under the National Recovery and Resilience Plan (NRRP), Mission 04 Component 2 Investment 1.5—NextGenerationEU, call for tender n. 3277 dated 30/12/2021, Award Number: 0001052 dated 23/06/2022.

REFERENCES

- [1] E. Commission, “REPowerEU: affordable, secure and sustainable energy for Europe.” Apr. 2022.
- [2] TERNA, “Progetto Pilota per Unità Virtuali Abilitate Miste - UVAM - Terna spa.” 2020.
- [3] F. Bovera and L. Lo Schiavo, “From energy communities to sector coupling: a taxonomy for regulatory experimentation in the age of the European Green Deal,” *Energy Policy*, vol. 171, p. 113299, 2022, doi: 10.1016/j.enpol.2022.113299.
- [4] E. Commission, “Making Our Homes and Buildings Fit for a Greener Future.” Apr. 2021.
- [5] J. Sánchez Ramos, M. Pavón Moreno, M. Guerrero Delgado, S. Álvarez Domínguez, and L. F. Cabeza, “Potential of energy flexible buildings: Evaluation of DSM strategies using building thermal mass,” *Energy Build*, vol. 203, p. 109442, Nov. 2019, doi: 10.1016/j.enbuild.2019.109442.
- [6] G. Reynders, T. Nuytten, and D. Saelens, “Potential of structural thermal mass for demand-side management in dwellings,” *Build Environ*, vol. 64, pp. 187–199, 2013, doi: 10.1016/j.buildenv.2013.03.010.
- [7] G. Reynders, R. A. Lopes, A. Marszal-Pomianowska, D. Aelenei, J. Martins, and D. Saelens, “Energy flexible buildings: An evaluation of definitions and quantification methodologies applied to thermal storage,” *Energy Build*, vol. 166, pp. 372–390, 2018, doi: 10.1016/j.enbuild.2018.02.040.
- [8] M. J.N, N. M. Mateus, and C. da, “Measured and modeled performance of internal mass as a thermal energy battery for energy flexible residential buildings,” *Appl Energy*, vol. 239, pp. 252–267, 2019, doi: 10.1016/j.apenergy.2019.01.200.
- [9] D. T. Nguyen and L. B. Le, “Joint optimization of electric vehicle and home energy scheduling considering user comfort preference,” *IEEE Trans Smart Grid*, vol. 5, no. 1, pp. 188–199, 2014, doi: 10.1109/TSG.2013.2274521.
- [10] B. Favre and B. Peuportier, “Application of dynamic programming to study load shifting in buildings,” *Energy Build*, vol. 82, pp. 57–64, 2014, doi: 10.1016/j.enbuild.2014.07.018.
- [11] Z. Wei and J. Calautit, “Predictive control of low-temperature heating system with passive thermal mass energy storage and photovoltaic system: Impact of occupancy patterns and climate change,” *Energy*, vol. 269, p. 126791, 2023, doi: 10.1016/j.energy.2023.126791.
- [12] A. Thavlov and H. W. Bindner, “THERMAL MODELS FOR INTELLIGENT HEATING OF BUILDINGS,” ICAE, 2012, p. A10591.
- [13] Y. Chen *et al.*, “Experimental investigation of demand response potential of buildings: Combined passive thermal mass and active storage,” *Appl Energy*, vol. 280, p. 115956, 2020, doi: 10.1016/j.apenergy.2020.115956.
- [14] L. M. P. Ghilardi, A. F. Castelli, L. Moretti, M. Morini, and E. Martelli, “Co-optimization of multi-energy system operation, district heating/cooling network and thermal comfort management for buildings,” *Appl Energy*, vol. 302, p. 117480, Apr. 2021, doi: 10.1016/j.apenergy.2021.117480.
- [15] W. Gu, J. Wang, S. Lu, Z. Luo, and C. Wu, “Optimal operation for integrated energy system considering thermal inertia of district heating network and buildings,” *Appl Energy*, vol. 199, pp. 234–246, 2017, doi: 10.1016/j.apenergy.2017.05.004.
- [16] A. Bischi *et al.*, “A detailed MILP optimization model for combined cooling, heat and power system operation planning,” *Energy*, vol. 74, pp. 12–26, Apr. 2014, doi: 10.1016/j.energy.2014.02.042.
- [17] M. Zatti, M. Gabba, M. Rossi, M. Morini, A. Gambarotta, and E. Martelli, “Towards the optimal design and operation of multi-energy systems: The ‘efficity’ project,” *Environ Eng Manag J*, vol. 17, pp. 2409–2419, Apr. 2018, doi: 10.30638/eemj.2018.239.
- [18] ANSI/ASHRAE, *Standard 55: 2017, Thermal Environmental Conditions for Human Occupancy*. ASHRAE, 2017.
- [19] F. Bovera, “United We Stand: How Aggregates of Distributed Energy Resources Can Shape the Future Energy System,” 2021.
- [20] TABULA, “Typology Approach for Building Stock Energy Assessment.” 2015.
- [21] ASHRAE, *2013 ASHRAE handbook - fundamentals*, SI edition. American Society of Heating Refrigerating and Air-Conditioning Engineers Inc., 2013.
- [22] P. Gabrielli, M. Gazzani, E. Martelli, and M. Mazzotti, “Optimal design of multi-energy systems with seasonal storage,” *Appl Energy*, vol. 219, pp. 408–424, Apr. 2018, doi: 10.1016/j.apenergy.2017.07.142.
- [23] GME, “GME - Statistiche - dati di sintesi MPE-MGP.” 2013.